

# Black hole spin in GRS 1915+105

Matthew Middleton<sup>1</sup>, Chris Done<sup>1</sup>, Marek Gierliński<sup>1,2</sup> and Shane W. Davis<sup>3</sup>

<sup>1</sup>*Department of Physics, University of Durham, South Road, Durham DH1 3LE, UK*

<sup>2</sup>*Observatorium Astronomiczne Uniwersytetu Jagiellońskiego, 30-244 Kraków, Orla 171, Poland*

<sup>3</sup>*University of California at Santa Barbara, California, USA*

8 September 2018

## ABSTRACT

Microquasars are galactic black hole binary systems with radio jets which can sometimes be spatially resolved to show superluminal motion. The first and best known of this class of objects is GRS 1915+105, the brightest accreting source in our Galaxy. There is persistent speculation that strong jet emission could be linked to black hole spin. If so, the high spin should also be evident in accretion disc spectra. We search the *RXTE* archive to find disc-dominated X-ray spectra from this object, as these are the only ones which can give reliable spin determinations by this method. Finding these is complicated by the rapid, unique limit cycle variability, but we are able to identify such spectra by going to the shortest possible time resolution (16 s). We fit them with a simple multicolour disc blackbody (DISKBB), and with the best current model which include full radiative transfer as well as relativistic effects (BHSPEC). Both these models show that the spin is intermediate, neither zero nor maximal. BHSPEC, the most physical model, gives a value for the dimensionless spin of  $a_* \sim 0.7$  for a distance of 12.5 kpc and inclination of  $66^\circ$ . This, together with the range of spins  $0.1 < a_* < 0.8$  derived using this method for other black holes, suggests that jet emission is probably fundamentally powered by gravity rather than spin, and implies that high-to-maximal spin is not a pre-requisite for powerful relativistic jets.

**Key words:** X-rays: binaries – black hole physics – accretion, accretion discs – stars: individual: GRS 1915+105

## 1 INTRODUCTION

Astrophysical black holes are very simple objects, completely characterized by their mass and spin. Mass can be measured using Newtonian mechanics by studying objects orbiting the black hole. For the Galactic black holes this is the companion star of the binary system, while for the supermassive black holes in galaxy nuclei this can be traced by nearby stars or gas in orbit around it. However, unlike mass, spin does not leave a discernable mark on the external spacetime at large distances. It only makes a significant difference close to the event horizon, so it is much more difficult to measure.

Since the spin of a black hole is generally not well known it becomes an obvious parameter to use to ‘explain’ any unusual behaviour. Jet production is a case in point. About 10 per cent of quasars are known to be radio loud, while the rest are radio quiet. Similarly, some of the Galactic black hole binaries are also known to produce relativistic jets (e.g. Fender, Belloni & Gallo 2004). There is persistent speculation in the literature that jet production is linked to the spin of the black hole (e.g. Moderski, Sikora & Lasota 1998). Theoretically, this could be due to direct tapping of the spin energy of the black hole via the Blandford-Znajek effect (Blandford & Znajek 1977). These ideas can only be directly tested by measuring the spin, so it becomes an important property to constrain.

The most obvious consequence of black hole spin is that it drags the last stable orbit inwards, from  $6R_g$  (where  $R_g \equiv GM/c^2$ , and  $M$  is the black hole mass) for a non-rotating black hole to  $1.23R_g$  for a maximal spin of  $a_* = 0.998$ , where dimensionless spin parameter  $a_*$  is defined as  $Jc/GM^2$ , and  $J$  is the black hole angular momentum. Thus for the same mass accretion rate through a disc, a spinning black hole has a higher disc luminosity and temperature. Equivalently, in terms of direct observables, a spinning black hole of the same luminosity has a higher disc temperature. However, using this to measure black hole spin is not entirely straightforward as black hole spectra are generally complex. The accretion disc spectrum is always accompanied by a tail of emission to much higher energies. While the origin of this tail is not well understood, it clearly points to some fraction of the energy being dissipated outside of the optically thick disc material, so that it does not thermalize. The tail can have a large impact on the derived disc luminosity and temperature if it carries a large fraction of the bolometric luminosity (see e.g. Kubota & Done 2004), so disc radii derived from these spectra are highly model dependent. Conversely, where the tail is not energetically important the disc spectrum can be reliably determined, and direct fitting of such disc dominated spectra can give an estimate for the black hole spin (e.g. Ebisawa et al. 1991; Gierliński, Maciołek-Niedźwiecki & Ebisawa

2001). However, a further problem is that the disc spectrum is not a simple sum of blackbody spectra from different radii. Distortions from Compton scattering from within the disc itself are probably important (Shakura & Sunyaev 1973; Shimura & Takahara 1995; Merloni et al. 2000; Davis et al. 2005), making this method dependent on the assumed vertical disc structure.

A variant on this method is to use a sequence of disc dominated spectra from a given source, at different luminosities. A constant radius disc at different mass accretion rate should have luminosity,  $L \propto T^4$  where  $T$  is the maximum temperature. The proportionality constant gives a measure of the disc area, and hence radius, modulo uncertainties in the spectral distortions introduced by Compton scattering in the disc itself. The advantage of this method is that observationally many sources show  $L \propto T^4$ , giving confidence in a well defined, constant inner disc radius to associate with the last stable orbit (Ebisawa et al. 1991, 1993; Kubota et al. 2001; Kubota & Makashima 2004; Kubota & Done 2004; Gierliński & Done 2004), and for an approximately constant colour temperature correction for the spectral distortions (Shafee et al. 2006; Davis, Done & Blaes 2006).

Here we apply this method to GRS 1915+105. This is the obvious source to use to investigate links between black hole spin and jet behaviour as it was the first galactic source to show a superluminal radio jet (Mirabel & Rodríguez 1994). Several more superluminal jet sources have since been found (GRO J1655–40, XTE J1748–288, V4641 Sgr), while a much larger number of black holes (together termed the microquasars) show jet-like radio morphology (e.g. Mirabel & Rodríguez 1999). Mildly relativistic jets are now recognized as a common feature of black holes at low mass accretion rates, while strong radio flaring is probably associated with state changes (e.g. Fender, Belloni & Gallo 2004).

However, GRS 1915+105 is also the most spectacularly variable accreting black hole in our Galaxy, showing episodes where it continually switches between states in a quasi-regular way (see e.g. the review by Fender & Belloni 2004 and references therein). Belloni et al. (1997a) showed that this variability could be associated with the accretion disc spectrum switching from hot and bright, implying a small inner disc radius, to cooler and dimmer, with a larger inferred radius. They interpreted this as the result of a limit-cycle instability in the inner accretion disc, such that it is continually emptying and refilling. Whatever its origin, this variability complicates the spectral analysis, as does the high absorbing column density towards this source. Nonetheless, by going to the highest resolution spectra (16 s) we are able to find disc dominated spectra, and these show an approximate  $L \propto T^4$  relation (see also Munro et al. 1999). We fit these spectra simultaneously with the best currently available theoretical accretion disc models (Davis et al. 2005) and find  $a_* \sim 0.7$  for a distance of 12.5 kpc. There are considerable uncertainties on the system parameters, but this spin is consistent with the moderate spins found from other, better constrained, GBH jet systems (Davis et al. 2006). We show this is also consistent with the most recent numerical MHD simulations of the accretion flow, which show that moderate spin black holes can produce powerful jets (Hawley & Krolik 2006; McKinney 2005).

## 2 SPECTRAL MODEL

We use XSPEC version 11.3 for spectral fitting. The main component of our model is emission from the optically thick accretion disc. For data selection (Section 3) and for some of the spectral modelling (Section 4.1) we use a multicolour disc blackbody,

DISKBB (Mitsuda et al. 1984). We also use more advanced model taking into account the spectral distortions from Comptonization in the disc and relativistic corrections in Section 4.2. The disc photons are Comptonized in optically thin plasma, for which we use thermal Comptonization model THCOMP (Zdziarski, Johnson & Magdziarz 1996; Życki, Done & Smith 1999). We also include a Gaussian (with energy constrained to be between 6–7 keV and  $\sigma$  fixed at 0.5 keV) and smeared edge (Ebisawa et al. 1991) to approximately describe the reflected emission. The Galactic absorption is modelled as in Done et al. (2004), i.e. with variable abundance cold gas VARABS with abundances from Anders & Ebihara (1982) and fixed column of  $N_H = 4.7 \times 10^{22} \text{ cm}^{-2}$  in all elements apart from Si and Fe, which had equivalent H column (assuming ISM abundances) of  $16.4 \times 10^{22}$  and  $10.9 \times 10^{22} \text{ cm}^{-2}$ , respectively, as determined from the *Chandra* Transmission Grating results of Lee et al. (2002).

We assume the black hole mass of  $14 M_\odot$  (Harlaftis & Greiner 2004), the disc inclination of  $66^\circ$  (Fender et al. 1999) and the distance to the source of 12.5 kpc (Rodríguez & Mirabel 1999), unless stated otherwise.

## 3 SELECTING DISC-DOMINATED SPECTRA

The derived disc temperature and luminosity are strongly model-dependent where the X-ray tail constitutes more than  $\sim 20$  per cent of the total bolometric power (e.g. Kubota & Done 2004). Hence it is very important to select only disc-dominated spectra to determine the black hole spin. We aim to choose only the spectra with less than 15 per cent contribution from Comptonization to the bolometric flux.

Another issue with data selection is the rapid variability seen in GRS 1915+105, where the spectrum switches rapidly between states with strong disc-like spectra (states A and B) and states with strong high-energy emission (state C; see Belloni et al. 1997, 2000). Spectra accumulated over long timescales (e.g. a single *RXTE* pointing, which is typically a few thousand seconds long) are quite often a mixture of states, so cannot be averaged together. Therefore, we can either extract spectra on much shorter timescales, shorter than the spectral variability timescale, or try to find longer periods with little variability.

### 3.1 Long timescale spectra

We first investigated longer timescales by accumulating spectra over entire pointed observations (designated by an identifier, obsid). We selected only stable data intervals with less than 5 per cent rms variability in light curves with 16-s resolution. There are some observations in which the source was only in the disc-like state A or B with very little variability. These were classified as variability states  $\phi$  and  $\delta$  by Belloni et al. (2000). However, they do not necessarily show disc-dominated spectra. We use the spectrum from obsid 10408-01-20-00 as an example of variability class  $\phi$  to illustrate the difficulties in fitting these spectra.

We extracted these data (all PCUs, all layers), together with background and response using FTOOLS 5.3 using standard extraction criteria. We added a 1 per cent systematic error in each energy channel to account for the residual uncertainties in the response. We fitted them with the model described in Section 2, using DISKBB for the disc emission. Fig. 1 shows our best-fitting deconvolution of this spectrum, together with residuals which are dominated by a known resonance absorption line (Kotani et al. 2000).

The continuum curvature is best described by a weak, low-temperature disc plus substantial amounts of Comptonized emission than by a disc alone. This could simply represent the effects of distortion by Compton scattering within the disc itself, but such strong distortions are not predicted by the best current disc models. These remain rather close to a DISKBB shape as long as the dissipation of gravitational potential energy occurs at more than a few optical depths within the disc (Davis et al. 2005).

Such low-temperature Comptonization contrasts with the usual spectral decomposition for the high/soft state in black hole binaries, where the spectrum can be dominated by the disc, with a weak Comptonized emission with photon spectral index of  $\Gamma \sim 2$ . However, high luminosity black hole binaries can also show an alternative type of spectrum, where the spectrum below 20 keV can be characterized by Comptonization with a temperature of 10–30 keV, together with the disc emission (very high state/steep power law state e.g. Kubota et al 2001; Kubota & Done 2004). The temperature inferred here is much lower, at  $kT_e \sim 3$  keV, but it could be a more extreme version of this state.

The energy dependence of the variability gives another argument for the reality of this low-temperature Comptonization component. Zdziarski et al. (2001; 2005) found similar spectral decompositions (disc plus low-temperature Comptonization) for apparently disc-like spectra from the  $\omega$  state of GRS 1915+105. They show that the rms variability spectrum for these data increases with energy, as predicted from models of a relatively stable disc and a more variable Comptonization component. Thus, it seems likely that even these apparently disc-like spectra are distorted by a (low temperature) Comptonization component. Since the disc luminosity and temperature can be significantly distorted in spectra with strong Comptonization (Kubota & Done 2004; Done & Kubota 2006), then these data cannot be used to give robust estimates of the disc properties.

We re-examined all the spectral fits of Done et al. (2004), which used all available *RXTE* observations before the end of Epoch 4 (up to 2000 May 11) and none of these had Comptonization which contributed less than 15 per cent of the bolometric flux. This was also the case with these data split into 128-s spectra. None of these data fit the criteria for being disc dominated, so none of them are suitable for disc spectral fitting.

### 3.2 Short timescale spectral binning

In Section 3.1 we have shown that there are no disc-dominated spectra (with Comptonization contribution less than 15 per cent) in the (stable) data accumulated on timescales longer than 128 s. The apparently disc-shaped spectra are instead dominated by low-temperature Comptonization. Therefore, we look at shorter timescales of 16 s (the timing resolution of Standard-2 data) and check if we can find disc-dominated spectra in the periods of larger variability on longer timescales, which were excluded from our previous analysis. As there still can be substantial variability over timescales shorter than 16 s (Belloni et al. 2000), we select only those variability classes where the characteristic switches between spectral states are rather slow (classes  $\beta$  and  $\kappa$  of Belloni et al. 2000). We selected 16 pointed observations of these, as detailed in Table 1.

We extracted PCA spectra in 16-s segments from Standard-2 data for each of these observations, using FTOOLS 5.3. We used all available PCUs and all the PCA layers and corrected the spectra for background and dead-time effects. No systematic uncertainties were added to the data as the short integration time gave

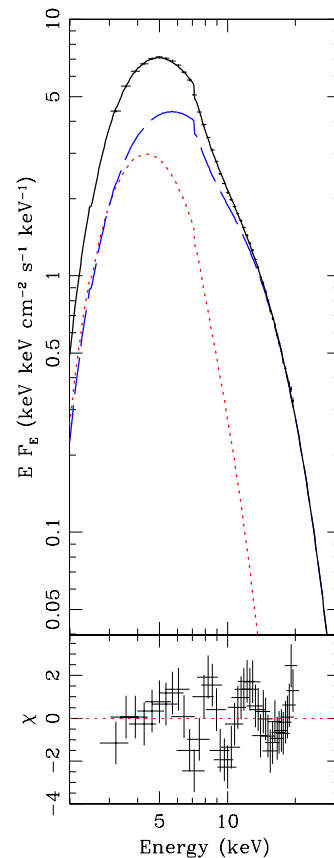


**Figure 1.** The apparently disc dominated spectrum of variability class  $\phi$  (obsid 10408-01-20-00). The best fitting spectral decomposition (using DISKBB and THCOMP) instead gives a low-temperature Comptonization component (long-dashed curve) as well as a disc (dotted curve). The total spectrum (solid curve) also includes a Gaussian line (short-dashed) and iron edge feature to roughly model the reflected emission. The lower panel shows residuals, which are dominated by traces of highly ionized absorption (Kotani et al 2000; Lee et al 2001).

statistical uncertainties which were always larger than  $\sim 1$  per cent in each channel. In order to ascertain the variability within 16-s intervals, we also extracted corresponding Standard-1 light curves with 0.125-s resolution, but no spectral resolution. We fitted each spectrum in XSPEC using the model described in Section 2, with DISKBB disc emission, and seed photon temperature independent of the disc temperature. We obtained acceptable fits, with reduced  $\chi^2_\nu < 1.3$ , for all  $\sim 4000$  spectra.

Removing absorption from each model fit gives the best estimate of the intrinsic spectrum of the source using these components. This model spectrum is then used to calculate intrinsic soft and hard colours (i.e. corrected for the effects of absorption and the instrument response), as in Done & Gierliński (2003). These are formed from the (energy) flux ratios of 4–6.4/3–4 keV and 9.7–16/6.4–9.7 keV, for the soft and hard colours, respectively. We also use the unabsorbed model spectrum to estimate the total bolometric luminosity from 0.01–1000 keV flux, for the distance of 12.5 kpc.

We use these fluxes to select data where the disc contributes more than 85 per cent of the total bolometric luminosity. However, not all of these spectra are necessarily appropriate to use for the disc analysis as the variability in GRS 1915+105 is extreme. The source can change significantly (in both spectral shape and normalization)

Class	Observation ID
$\beta$	10408-01-10-00, 10408-01-21-00, 20402-01-43-00, 20402-01-43-02, 20402-01-44-00, 20402-01-45-00 20402-01-45-03, 20402-01-46-00, 20404-01-52-01, 20402-01-53-00, 20402-01-59-00
$\lambda$	10408-01-37-00, 10408-01-38-00, 20402-01-36-00, 20402-01-36-01, 20402-01-37-01

**Table 1.** Observation IDs (obsids) from variability classes  $\beta$  and  $\kappa$  (Belloni et al. 2000) where transitions between apparently disc dominated and Comptonized spectra are slow enough to be potentially resolved by the 16-s time resolution data from Standard-2 data.

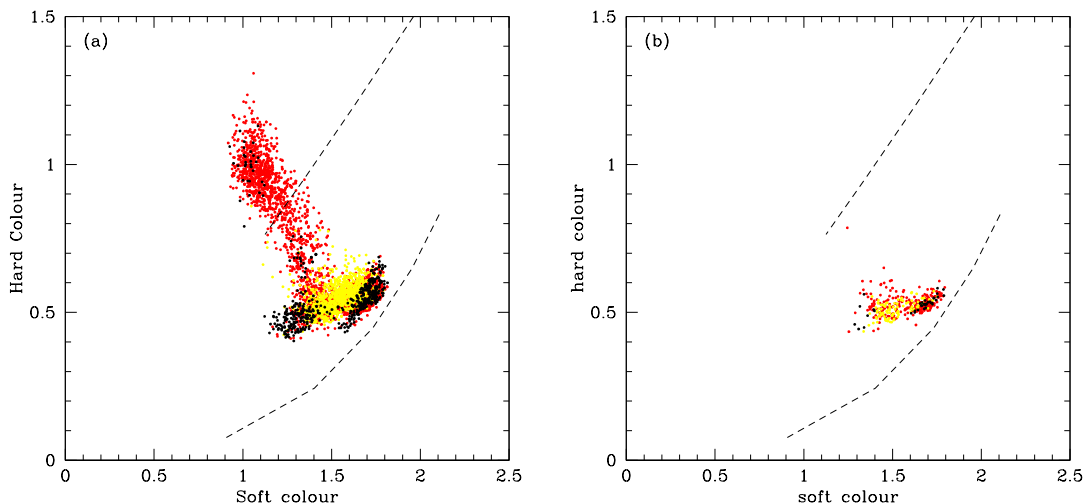


**Figure 2.** Colour-colour diagrams for the spectra extracted in 16-s intervals. Red points are spectra with 50 per cent or more rms variability, yellow between 50 and 20 per cent rms, while black is less than 5 per cent. (a) Colours calculated from all observations listed in Table 1. (b) A subset of the entire sample, limited to the disc-dominated spectra, with less than 15 per cent of the bolometric luminosity in the hard tail. The diagonal dashed line indicates the range of colours from a power-law spectrum with index varying from 1.5 (top right) to 3.0 (bottom left) while the lower curve indicates the colours expected from a disc dominated spectrum at different temperatures, derived from DISKBB with temperature 1–3 keV. We chose only disc-dominated spectra with less than 5 per cent rms variability—black points in panel (b)—for detailed analysis.

on timescales shorter than 16 s. The spectra accumulated over such intervals can be severely distorted, even if they consist only of a pure disc varying in temperature. Hence, we fold in an additional selection criteria, which is that the rms variability during each 16-s interval should be less than 5 per cent. We use the 0.125-s resolution Standard-1 light curves corresponding to each 16-s spectrum to calculate the rms amplitude.

Fig. 2 illustrates our data selection on a colour-colour diagram. The dashed lines show the intrinsic colours expected for a power law and pure disc spectrum (upper and lower curves, respectively). Fig. 2(a) shows all the data, where red, yellow and black points indicate an rms variability of 50–20, 20–5 and less than 5 per cent, respectively. Fig. 2(b) shows the same diagram for those spectra where the disc is dominant (where the tail is less than 15 per cent of the total bolometric luminosity). As expected, these all lie fairly close to the spectrum of a disc (lower dashed curve) as opposed to a power law (upper dashed straight line), but some are still quite variable, so could be a mix of states and/or disc temperatures. Hence we only use spectra where there is less than 5 per cent rms variability (black points), leaving a total of 34 disc-dominated, steady spectra across 6 obsids with which we carry out our analysis (Table 2).

## 4 DISC DOMINATED, STEADY SPECTRA

### 4.1 DISKBB model results

Each disc dominated spectrum was refit using the same model as before except that the seed photons for the Comptonization are now tied to those of the disc since these spectra are disc dominated. The derived disc parameters (temperature and flux) are used to plot a luminosity-temperature ( $L$ - $T$ ) diagram as in GD04. We corrected the DISKBB temperature and flux from each spectrum for the effects of disc geometry and relativistic smearing (assuming a given spin and inclination of  $66^\circ$ ), plus an additional correction to incorporate a stress-free inner boundary condition (which is not included in DISKBB). Then, we converted this to a luminosity using the assumed distance of 12.5 kpc. These corrected data points can then be compared with the theoretically expected  $L$ - $T$  plot for the assumed mass ( $14 M_\odot$ ) and spin (correction factor interpolated for an inclination of  $66^\circ$  from the tabulated values of Zhang et al. 1997) of the black hole, for an assumed colour temperature correction of 1.8 (Shimura & Takahara 1995) to relate the observed temperature which is distorted by Compton scattering to the equivalent black-body temperature.

Figs 3(a) and (b) show the corrected data and expected model  $L$ - $T$  relation for zero and maximal spin. Plainly the data follow an approximate  $L \propto T^4$  relation as expected from constant radius disc, and equally plainly the data suggest the spin is intermediate, rather than zero or maximal.

Model component	Parameter	spectrum (a)	spectrum (b)	spectrum (c)
DISKBB	$T_{\text{in}}$ (keV)	$1.337^{+0.004}_{-0.002}$	$1.71^{+0.02}_{-0.05}$	$1.92^{+0.04}_{-0.05}$
	$R_{\text{in}}$ (km)	$38.0^{+1.3}_{-0.7}$	tied	tied
THCOMP	$\Gamma$	$2.53^{+0.39}_{-0.22}$	$1.04^{+0.32}_{-0.03*}$	$1.25^{+0.29}_{-0.24*}$
	$kT_e$ (keV)	$3.75^{+0.68}_{-0.55}$	$2.90^{+0.13}_{-0.18}$	$2.59^{+0.13}_{-0.10}$
	$\chi^2_\nu$	133.6/113		
BHSPEC	$L_{\text{disc}}/L_{\text{Edd}}$	$0.524^{+0.007}_{-0.005}$	$0.96^{+0.01}_{-0.15}$	$1.52^{+0.22}_{-0.08}$
	$a_*$	$0.720^{+0.009}_{-0.017}$	tied	tied
THCOMP	$\Gamma$	$1.01^{+0.25}_{-0.17}$	$1.22^{+0.42}_{-0.21*}$	$3.1^{+0.7}_{-0.9}$
	$kT_e$ (keV)	$2.51^{+0.17}_{-0.05}$	$3.28^{+0.22}_{-0.23}$	$8.8^{+9.1*}_{-4.5}$
	$kT_{\text{bb}}$ (keV)	(1.34)	(1.71)	(1.92)
	$\chi^2_\nu$	143.8/113		

**Table 3.** Best-fitting parameters for the 3 representative spectra fitted simultaneously with the model consisting of the disc emission and thermal Comptonization. The black hole mass of  $14 M_\odot$ , the disc inclination of  $66^\circ$  and the distance of 12.5 kpc were assumed (where applicable). In the model with DISKBB the inner disc radius,  $R_{\text{in}}$ , is calculated from the DISKBB normalization, without any colour or relativistic corrections. In the model BHSPEC the seed photon temperature was fixed at the best-fitting values of the DISKBB model. The inner disc radius in DISKBB and the spin parameter in BHSPEC were tied across the three spectra. An asterisk denotes the parameter reaching its hard limit within the error bar. The  $\chi^2_\nu$  quoted is for all three spectra fitted together.

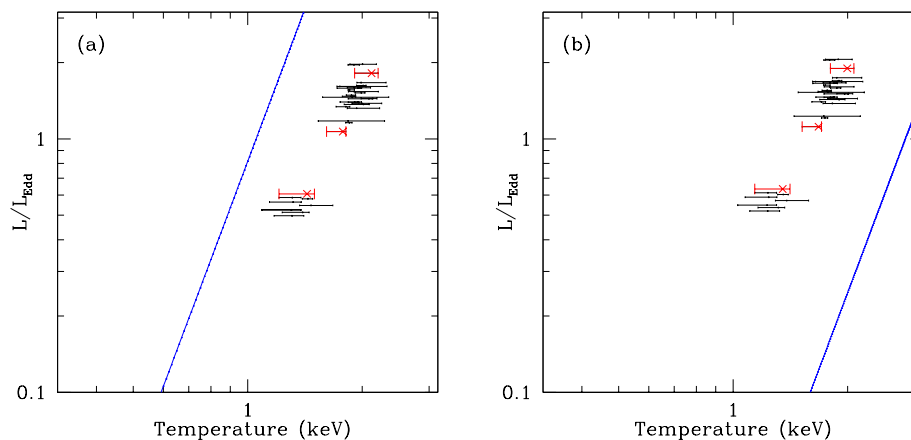


**Figure 3.** Luminosity-temperature plots for our sample of disc-dominated data with less than 5 per cent rms variability. (a) The intrinsic disc luminosity and temperature (data points) derived assuming a Schwarzschild black hole (Zhang, Cui & Chen 1997). The solid line represents the expected  $L \propto T^4$  relation. (b) The same data points, but corrected for maximal Kerr spin with the corresponding  $L \propto T^4$  relation expected for the much smaller disc inner radius. Plainly the data lie between these two extreme values. The points highlighted by diagonal crosses indicate the data selected for further spectral fitting. These span the entire luminosity range and are representative of the source behaviour so can be used to determine the black hole spin.

We can explicitly test how well the source follows the  $L \propto T^4$  relation i.e. whether the emission is consistent with a constant inner radius disc (with constant colour temperature correction) by fitting several of the disc spectra simultaneously within XSPEC, with the disc inner radius tied across all data sets. We select 3 of the disc-dominated spectra, shown by the diagonal crosses in Fig. 3, encompassing the spread in luminosity seen from the disc. When fit separately these give a total  $\chi^2_\nu = 127.2/111$ , while when fit simultaneously, with the DISKBB normalization ( $\propto r^2$ ) tied across all 3 data sets gives 133.6/113. Thus the 3 data sets are completely statistically consistent with a constant radius, constant colour temperature corrected disc spectrum. The results are shown in Table 3.

## 4.2 BHSPEC model results

The spectral model DISKBB assumes that each point of the disc emits as a blackbody. In practice, the local spectrum is more com-

plex. At low frequencies true absorption opacity dominates and the emission is blackbody, but for higher frequencies, electron scattering opacity is larger leading to departures from local thermodynamic equilibrium and producing a modified blackbody spectrum (see e.g. Shakura & Sunyaev 1973). Also, the absorption opacity has significant contributions from free-bound (photo-electric edges) as well as free-free which again give frequency dependent effects on the radiative transfer. BHSPEC (now publicly available<sup>1</sup> as an XSPEC table model) utilizes a self-consistent calculation of the spectrum including all these radiative transfer effects as a function of inclination (Davis et al. 2005). BHSPEC also incorporates the relativistic effects and inner boundary condition directly in the model.

We use the same 3 spectra as before and fit them using BH-

<sup>1</sup> BHSPEC can be downloaded from <http://heasarc.gsfc.nasa.gov/docs/xanadu/xspec/newmodels.html>

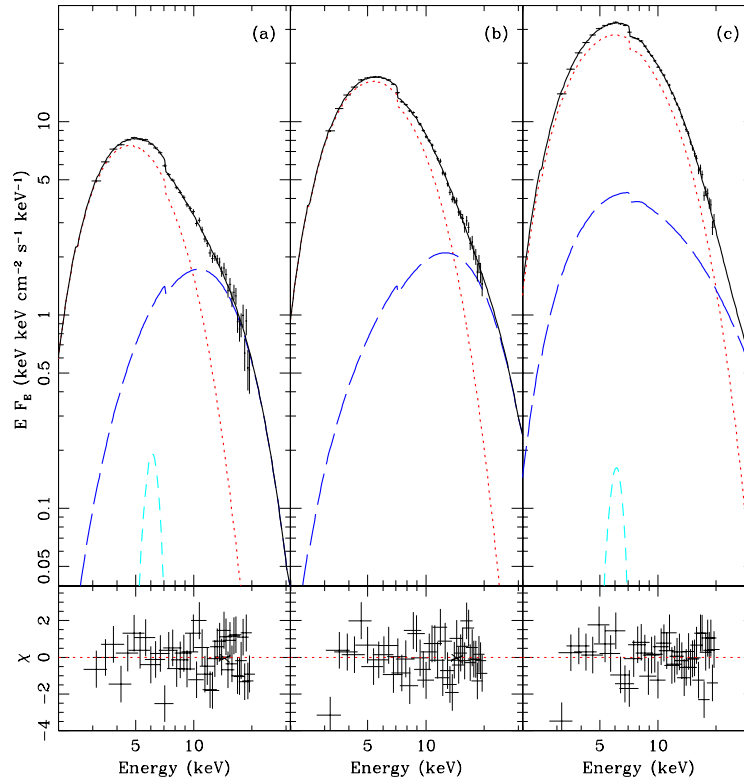


**Figure 4.** Individual fits of BHSPEC of the 3 ultrasoft spectra which encompass the observed range in luminosity of disc dominated spectra. The 3 plots beneath each spectrum show the respective residuals for each fit. The data (black points) are fit by a model consisting of the BHSPEC disc spectrum (red line), its Comptonized emission (blue line) and Gaussian iron line (cyan line) giving a total spectrum (black line).

SPEC as the disc component (Fig. 4), assuming the viscosity parameter  $\alpha = 0.01$  (Davis et al. 2006). We fixed the seed photon temperature in the Comptonization model to that of the previous DISKBB fits, as BHSPEC is parameterized by mass accretion rate rather than by temperature. This gives  $\chi^2_{\nu} = 143.8/113$  and  $a_* = 0.720^{+0.009}_{-0.017}$ . The fit results are shown in Table 3.

We note that the fit using BHSPEC is marginally worse than the fit using DISKBB. This is because the relativistic corrections included in BHSPEC give a slightly different spectral shape than DISKBB and the data slightly prefer a Wien shape to the relativistically distorted Wien. However, at this level there are other approximations which can also affect the spectrum, such as the amount of returning radiation illuminating the disc and the spectral shape of the seed photons assumed for the Comptonized emission (see also Davis et al. 2006).

### 4.3 System Parameter Uncertainties

The fits above all assume a distance of 12.5 kpc. However, this is not well determined, and estimates range from this to as low as 7 kpc, though 11 kpc is the only distance which is compatible with all the constraints (see e.g. Zdziarski et al. 2005). We investigate the effect this uncertainty has on the spin estimates by refitting the spectra with these distances within the BHSPEC model. We find that the distance simply trades off against the inferred spin and luminosity giving  $a_* = 0.990_{-0.005}$  (there is no upper limit as the BHSPEC model table we use only includes values of spin up to 0.99) and  $0.819^{+0.005}_{-0.007}$ , for the distance of 7 and 11 kpc, respectively.

The most likely mass of the source is  $14 \pm 4 M_{\odot}$  (Harlaftis &

Greiner 2004). It is highly unlikely that this mass is an overestimate as the source would be even more super Eddington at lower masses, however an underestimate is possible if the jet axis is misaligned. To address this uncertainty we tested the effect on the spin parameter with mass frozen at the upper limit of  $19 M_{\odot}$ . Fitting the same spectra as before a spin value of  $0.88 \pm 0.01$  is obtained.

The inclination of the jet has remained constant to within a few degrees for several years (Fender et al. 1999). This motivates the belief that the jet is perpendicular to the axis of the disc. The value of Fender et al. (1999) of  $(66 \pm 2)^{\circ}$ , as determined through MERLIN observations, provides the best estimate for the inclination of the system. However, the upper limit of the eclipsing angle, determined to be  $79^{\circ}$  (Greiner et al. 2001) yields a useful lower limit to the spin through fitting the same three spectra of  $0.10^{+0.04}_{-0.07}$ .

## 5 ALTERNATIVE SPIN DETERMINATIONS

### 5.1 Disc spectral fitting

McClintock et al. (2006) similarly study the spin of GRS 1915+105 from a much larger sample of *RXTE* data, but find rather different results. Their inferred spin is luminosity-dependent, with low-luminosity data predicting maximal spin, while at higher luminosities,  $\gtrsim 0.4 L_{\text{Edd}}$ , the measured spin gradually decreases, with their high-luminosity spin measurements being comparable with our results. They argue that the low luminosity results are more robust due to theoretical uncertainties on the disc structure at high luminosities. It is certainly true that there are many uncertainties on calculating disc structure at luminosities close to Eddington and



Observation ID	Start time (s)	Stop time (s)	Selection
10408-01-10-00	75749539	75749555	
(Class $\beta$ )	75755491	75755507	
	75755507	75755523	
	75756499	75756515	
	75756947	75756963	(b)
10408-01-21-01	79325363	79325379	
(Class $\beta$ )	79325395	79325411	
	79325459	79325475	
	79325475	79325491	
	79325491	79325507	
10408-01-38-00	87288867	87288883	
(Class $\lambda$ )	87289779	87289795	
	87290083	87290099	
	87290131	87290147	
	87293843	87293859	
	87293891	87293907	
	87293923	87293939	
	87293971	87293987	
	87295075	87295091	
	87295987	87295991	(c)
	87296051	87296067	
	87296179	87296195	
	87296211	87296227	
	87299347	87299363	
	87299363	87299379	
	87300275	87300291	
	87300387	87300403	
20402-01-45-03	116410403	116410419	
(Class $\beta$ )	116410419	116410435	
	116410435	116410451	
	116417059	116417075	(a)
20402-01-59-00	124956003	124956019	
(Class $\beta$ )	124957043	124957059	

**Table 2.** Log of 16-s disc-dominated spectra with less than 5 per cent variability, used for spectral fitting in Section 4. Start and stop times are in mission elapsed time, which is number of seconds since 1994 January 1, 0<sup>h</sup>0<sup>m</sup>0<sup>s</sup> UTC. They are represented by black points in Fig. 2(b). The last column indicates the three spectra selected for spectral analysis in Section 4, and indicated by diagonal crosses in Fig. 3

above. However, the lower luminosity spectra are affected by uncertainties in spectral modelling. McClintock et al. (2006) used several different descriptions of the Comptonized emission (power law, COMPTT and exponentially cutoff power law), but none of these allowed for the possibility of a temperature as low at  $\sim 3$  keV (see Section 3.1)

We illustrate the limitations of this approach by refitting one of their spectra (obsid 10408-01-20-00, as in Section 3.1) using a model very similar to theirs, consisting of BHSPEC and COMPTT, Galactic absorption, broad absorption line, smeared edge, and an additional narrow edge at  $\sim 8$  keV. Following McClintock et al. (2006) we have fixed the seed photon temperature for Comptonization at 2.0 keV and electron temperature at 50 keV. We obtained a good fit ( $\chi^2_\nu = 38.0/36$ ), where the spectral decomposition is dominated by the disc (Fig. 5a). The high disc temperature then requires a high spin. However, a better fit is obtained by allowing the electron temperature to be free, giving  $\chi^2_\nu = 13.0/35$  (showing the effect of the systematic rather than statistical uncertainties).

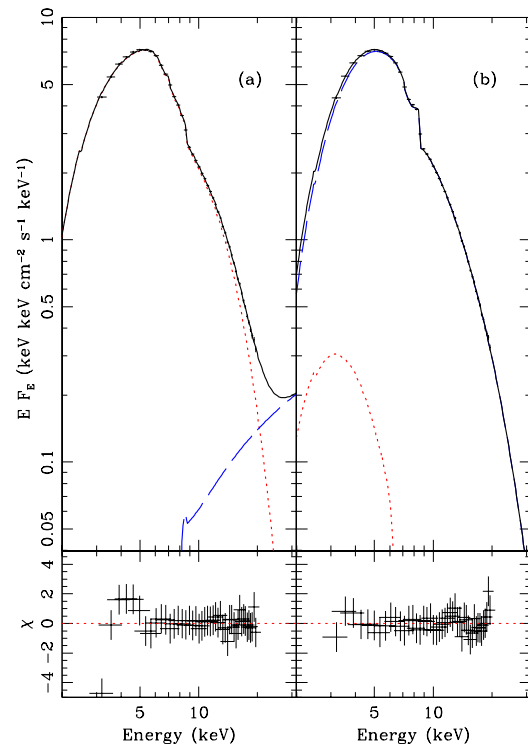


**Figure 5.** Fits for obsid 10408-01-20-00 using BHSPEC and COMPTT with the electron temperature fixed at 50 keV (a) and free (b). The plots beneath each spectrum show the respective residuals for each fit. The data (black points) are fit by a model consisting of the BHSPEC disc spectrum (dotted curve), its Comptonized emission (dashed curve) giving a total spectrum (solid line) without an Gaussian iron line in either case.

The spectrum is then dominated by the low-temperature Comptonized component (similar to the one shown in Fig. 1), where the disc contributes only 10 per cent of the flux and is at much lower temperature (Fig. 5b). The derived Comptonization temperature is  $3.25^{+0.41}_{-0.58}$  keV (where the limits are 90 per cent confidence on one free parameter, i.e.  $\Delta\chi^2/\chi^2_\nu = 2.7$ , or  $\Delta\chi^2 = 7.27$ ). The upper limit is far below the values assumed by McClintock et al. (2006). The spin is not constrained now (see Table 4) and thus is consistent with our value derived in Sec. 4. This shows that the derived spin is dependent on the details of the data analysis, contrary to the robustness claimed by McClintock et al. (2006).

## 5.2 Broad iron line

A completely different method to potentially determine the spin is via relativistic broadening of the iron line and Compton reflection features (see e.g. the review by Fabian et al. 2000). Unlike the disc spectrum method, this depends on having a strong X-ray tail in order to pick out its reflection. Results from this are currently confused, mostly because the line is very variable. Most observations show that the line is not highly smeared, so the inner radius of the line emitting material is  $\gg R_g$  and hence cannot constrain the spin (e.g. Martocchia et al. 2002, 2004; Sobolewska & Życki 2003). However, there is one *BeppoSAX* observation where the derived line is extremely smeared, with the inner disc radius  $R_{\text{in}} = 1.4^{+3.7}_{-0.2} R_g$ , so requires a highly spinning black hole (Martocchia et al. 2004). This changing smearing on the line could be due to real changes in the disc inner radius, as required in the limit

cycle instability models for this source where the disc empties and refills (e.g. Belloni et al. 1997). It could also be due to changes in ionization of a constant radius disc. A third possibility is that the extreme smearing inferred from some spectra are actually artifacts of ionized absorption (Done & Gierliński 2005) which is known to be present in this source (Kotani et al. 2000; Lee et al. 2002). None of these are mutually exclusive, but whatever the cause, our best estimate of the spin of  $a_* = 0.7$  implies  $R_{\text{in}} = 3.4R_g$  so it is consistent (within the uncertainties) on even on the most extreme inferred smearing of the iron line.

### 5.3 Quasi-Periodic Oscillations

Yet another constraint on the properties of the innermost parts of the accretion flow is via the variability behaviour on short timescales. There are a number of quasi periodic oscillations (QPOs) which can be seen in the power spectra of the Galactic black hole binaries. The strongest of these is generally the low-frequency (LF) QPO, which moves in frequency, typically between 0.5–10 Hz. The properties of this feature are correlated with the spectral shape. In general it is seen when the spectrum consists of both a strong disc and strong X-ray tail, and the LF QPO frequency increases as the spectrum softens (e.g. Munro, Morgan & Remillard 1999). This feature can be both strong and sharp, so giving a clear observational diagnostic. The problem is that there is no widely accepted theory for QPO generation, though all current models require some moving characteristic radius in the disc to generate the changing frequency of the LF QPO. One of the promising approaches is to identify the LF QPO frequency with the precession frequency of a vertical perturbation in the flow, which depends on both the characteristic radius at which the QPO is produced, and black hole spin (Stella & Vietri 1999). Munro et al. (1999) show that the LF QPO spans 0.5–10 Hz in GRS 1915+105, so the maximum frequency must be produced by a disc with radius larger or equal to the last stable orbit. This only limits the spin to be  $a_* > 0.3$  (using the full expression for Lens-Thirring precession in Merloni et al. 1999) or  $a_* > 0.2$  if the LF QPO is at twice the precession frequency.

A more direct measure of black hole spin may be given by the high-frequency (HF) pair of QPO features which seem fairly fixed in frequency and in a 3:2 harmonic relation (though in GRS 1915+105 the frequency ratio are 3.36:2, so not exact; Strohmayer 2001). Harmonics are most naturally associated with a resonance in the disc, but again there are several possibilities for this resonance so as yet no unique way to translate these frequencies into black hole spin. Török et al. (2005) review the possible orbital resonances in a thin disc, and highlight the parametric resonance between vertical and radial epicyclic modes in strong gravity as these rather naturally give a 3:2 ratio (Kluźniak & Abramowicz 2002). This identification implies  $a_* = 0.9\text{--}0.98$  for the observed HF QPOs in GRS 1915+105. However, there are other resonances even in a thin disc which can also give a 3:2 ratio, though these generally predict other harmonics as well. Depending on which of these is chosen as the origin for the HF QPOs gives a value for the spin spanning the whole range from  $a_* = 0\text{--}0.998$  (Török et al. 2005). Another, perhaps more attractive possibility, is that the HF QPO is a resonance in a *thick* disc, where there are additional modes available from compression and extension of the disc scale height (breathing modes). Blaes, Arras & Fragile (2006) show that a ‘natural’ 3:2 resonance forms between the vertical epicyclic mode and a ‘breathing’ mode (Blaes, Arras & Fragile 2006). This identification gives much weaker constraints on spin than the parametric resonance.

The dispersion of values for the spin does not look promis-

ing and obviously all the techniques covered here have differing strengths and weaknesses. For the spectral methods, the physical origin of the features (disc or iron line) is clear, and the uncertainties are due to the observations, or rather how to unambiguously isolate the disc emission or relativistic line profile in a complex spectrum. Conversely, the timing methods are unambiguous observationally, but lack a theoretical model to uniquely associate the measured frequencies with black hole spin. Nonetheless, from this brief review it is clear that only potentially significant conflict with moderate ( $a_* = 0.7$ ) spin in GRS 1915+105 for a reasonable distance is the parametric resonance interpretation of the HF QPO which requires  $a_* \gtrsim 0.9$ , while the newer interpretation of this as the resonance between the vertical epicyclic and ‘breathing’ modes is consistent with any spin.

We note that the parametric resonance between the radial and vertical epicycles interpretation of the HF QPOs also gives a much higher spin for GRO J1655–40 and XTE J1550–564 of  $a_* \sim 0.96$  (Török et al 2005) than are derived from their disc spectrum,  $a_* \sim 0.7$  (Shafee et al. 2006) and  $a_* \sim 0.1$  (Davis et al. 2006), respectively. There are no issues in these sources with the strong variability or interstellar absorption, and the distances are rather better determined, so there seems to be a clear discrepancy between the results of the parametric resonance interpretation of the HF QPOs and the disc spectra. Again, this conflict is removed if the HF QPO is instead a resonance between the vertical epicyclic and breathing modes (Blaes et al. 2006).

## 6 BLACK HOLE SPIN AND JET POWER

One of the big questions in understanding accretion flows is how the jet is powered, whether it predominantly taps the gravitational potential or whether it predominantly taps the spin energy plausibly via the Blandford-Znajek mechanism. The possibility of spin powered jets has given rise to persistent speculation in the literature that relativistic jets require a maximally spinning black hole. GRS 1915+105 is the most powerful X-ray binary jet source in our Galaxy, so is a key object for testing models of jet formation. Our fits to the disc-dominated spectra from this source clearly show that the spin is unlikely to be maximal, though it is substantial ( $a_* = 0.7\text{--}0.8$  for any reasonable distance estimate). The same technique (simultaneous fitting of a series of disc dominated spectra at differing luminosities) gives non-maximal spins ( $a_* = 0.1\text{--}0.8$ ) for four other Galactic black holes (Davis et al. 2006; Shafee et al. 2006). These objects also show radio jets, sometimes with superluminal motion, so it is clear that these results imply that powerful jets do not require maximally spinning black holes.

The next question is whether spin is needed at all in producing a jet, i.e. whether the jet can be purely powered by gravity. Observationally it is clear that the jet power scales with accretion rate (Gallo, Fender & Pooley 2003). Since all the Galactic black holes are more or less consistent with the same ratio of radio to X-ray power (which traces the jet to accretion power) at a given  $L/L_{\text{Edd}}$  (in the hard spectral state), then the observed range of  $a_* = 0.1\text{--}0.8$  implies that the ratio of jet to accretion power does not depend strongly on spin. This immediately favours gravity powered jets, as spin powered jet models generically depend rather strongly on spin!

The best current jet models are those which are produced in numerical simulations of the jet/accretion flow. These include the self-consistent, magnetically generated stresses and produce jets and outflows without additional physics. These show in general that



Model component	Parameter	(a)	(b)
BHSPec	$L_{\text{disc}}/L_{\text{Edd}}$	$0.344^{+0.003}_{-0.004}$	$0.03^{+0.03}_{-0.02}$
	$a_*$	$0.990^{+0*}_{-0.002}$	$0.91^{+0.08*}_{-0.91*}$
COMPTT	$T_0$ (keV)	(2.0)	(1.0)
	$kT_e$ (keV)	(50)	$3.25^{+0.41}_{-0.48}$
	$\tau$	$1.6^{+5.6}_{-1.2}$	$2.6^{+0.8}_{-0.2}$
	Normalization	$8.3^{+15}_{-0.9} \times 10^{-4}$	$1.33^{+0.25}_{-0.15}$
	$\chi^2_\nu$	38.0/36	13.0/35

**Table 4.** Best-fitting parameters with errors for the two fits of obsid 10408-01-20-00 with (a) electron temperature fixed as in McClintock et al. (2006) and (b) free to vary. Note that the seed photon temperature ( $T_0$ ) is fixed to the value of McClintock et al. (2006) at 2 keV for (a) but we use 1 keV in our model (b) as this is more appropriate for the much lower luminosity inferred for the disc. Values in parentheses denote fixed parameters. An asterisk denotes the parameter reaching its hard limit within the error bar. As the reduced  $\chi^2$  in model (b) was much less than one, the errors were calculated for  $\Delta\chi^2/\chi^2_\nu = 2.7$ , i.e.  $\Delta\chi^2 = 7.27$ .

the jet has two components, a matter dominated, funnel wall jet and an electromagnetic Poynting flux jet (McKinney 2005; Hawley & Krolik 2006). The electromagnetic jet is probably highly relativistic with bulk Lorentz factor  $\gg 1$ , and is very strongly dependent on  $a_*$ , indicating that this may be partly (or perhaps even mostly) powered by the black hole spin (McKinney & Gammie 2004). By contrast, the funnel wall jet is less relativistic (perhaps only Lorentz factors  $\leq 2-3$ ) and is much less dependent on black hole spin (McKinney 2005; Hawley & Krolik 2006). The potential power of the matter jet relative to the accretion power increases by only a factor 2 between  $a_* = 0.5$  and 0.95 (Hawley & Krolik 2006). Such a small change is unlikely to result in much scatter in the observed ratio of radio to X-ray luminosity, in contrast with the factor 11 for the Poynting flux jet (Hawley & Krolik 2006). While we caution that the simulations do not currently include radiation, so cannot yet be unambiguously connected to observations, it seems that the funnel wall, matter dominated jet, powered predominantly by the gravity of the accretion flow, matches rather well to the properties of the jets in Galactic black hole binaries in that it can accommodate the observed constancy of radio to X-ray flux at a given  $L/L_{\text{Edd}}$  from objects with the variety of spins inferred here (see McKinney 2005).

The moderate spins derived from the disc spectra (as opposed to the near maximal spins derived from the HF QPOs: Török et al. 2005) also match with the theoretical predictions for the birth spin distribution of black holes, as the pre-supernovae core before stellar collapse is slowly rotating, and spin up from captured fallback of material is countered by angular momentum loss in gravitational waves during the formation process (see e.g. the review by Gammie, Shapiro & McKinney 2004). Spin-up through accretion during the lifetime of the binary is limited in most systems as the companion mass is generally smaller than the black hole mass (King & Kolb 1999).

## 7 CONCLUSIONS

We have searched the *RXTE* spectra from GRS 1915+105 to find the rare disc-dominated states. These can only be found at the shortest PCA (Standard-2 data) timescales of 16 s, as such spectra are seen only during the unique limit cycle variability of this source. We fit these with the best current models of the accretion disc spectrum, which include full radiative transfer through a solar abundance atmosphere as well as the full relativistic dissipation (with stress free inner boundary condition) and ray tracing to incorporate the relativistic effects on propagation of the emission (Davis et al.

2005; Davis & Hubeny 2006). This gives the spin of the black hole as  $a_* \sim 0.7$ , assuming the best current estimate for distance and binary system parameters. This, together with spins determined using this method for other galactic black holes gives a distribution of  $a_* \sim 0.1-0.8$  i.e. low-to-moderate spin. Moderate (as opposed to maximal) spins are consistent with theoretical expectations of the spin distribution of galactic black holes, and with the jet properties, but conflict with the high-to-maximal spin inferred (often for the same objects) from the broad iron line profile and parametric vertical-radial epicyclic resonance interpretation of the HF QPOs. While the broad line profile may be distorted by highly ionized absorption lines (Done & Gierliński 2006), the discrepancy between the spins derived from disc spectra and those derived from the vertical-radial epicyclic resonance interpretation of the HF QPO appears robust. Given the apparent simplicity of the accretion disc behaviour, it seems most likely that the HF QPO should instead be associated with another resonance in the disc, plausibly the vertical epicycle-breathing resonance identified by Blaes et al. (2006).

## ACKNOWLEDGEMENTS

We thank Jean-Pierre Lasota and Steve Balbus for useful discussions on the difference between spin and gravity powered jets. We also thank Julian Krolik and Jon McKinney for their help in understanding how to interpret the results of the MRI simulations. The editors of MNRAS probably deserve the undying gratitude of the readers for objecting to the wretched pun of the original title of ‘The spin of GRS 1915+105: why do we Kerr?’

## REFERENCES

- Anders E., Ebihara M., *Geochimica et Cosmochimica Acta*, 1982, 46, 2362
- Belloni T., Méndez M., King A. R., van der Klis M., van Paradijs J., 1997, *ApJ*, 488, L109
- Belloni T., Klein-Wolt M., Méndez M., van der Klis M., van Paradijs J., 2000, *A&A*, 355, 271
- Blandford R. D., Znajek R. L., 1977, *MNRAS*, 179, 433
- Blaes O. M., Arras P., Fragile P. C., 2006, *MNRAS*, 369, 1235
- Davis S. W., Blaes O. M., Hubeny I., Turner N. J., 2005, *ApJ*, 621, 372
- Davis S. W., Hubeny I., 2006, *ApJS*, 164, 530
- Davis S. W., Done C., Blaes O., *ApJ*, submitted
- Done C., Gierliński M., 2003, *MNRAS*, 342, 1041
- Done C., Gierliński M., 2005, *MNRAS*, 364, 208
- Done C., Gierliński M., 2006, *MNRAS*, 367, 659
- Done C., Kubota A., 2006, *MNRAS*, submitted, astro-ph/0511030

- Done C., Wardziński G., Gierliński M., 2004, MNRAS, 349, 393
- Ebisawa K., Mitsuda K., Hanawa T., 1991, ApJ, 367, 213
- Ebisawa K., Ueda Y., Done C., 1993, AAS, 25, 1381
- Fabian A. C., Iwasawa K., Reynolds C. S., Young A. J., 2000, PASP, 112, 1145
- Fender R. P., Garrington S. T., McKay D. J., Muxlow T. W. B., Pooley G. G., Spencer R. E., Stirling A. M., Waltman E. B., 1999, MNRAS, 304, 865
- Fender R. P., Belloni T. M., Gallo E., 2004, MNRAS, 355, 1105
- Gallo E., Fender R. P., Pooley G. G., 2003, MNRAS, 344, 60
- Gammie C. F., Shapiro S. L., McKinney J. C., 2004, ApJ, 602, 312
- Gierliński M., Done C., 2004, MNRAS, 347, 885
- Gierliński M., Maciołek-Niedźwiecki A., Ebisawa K., 2001, MNRAS, 325, 1253
- Greiner J., Cuby J. G., McCaughrean M. J., 2001, Natur, 414, 522
- Harlaftis E. T., Greiner J., 2004, A&A, 414, L13
- Hawley J. F., Krolik J. H., 2006, ApJ, 641, 103
- King A. R., Kolb U., 1999, MNRAS, 305, 654
- Kluźniak W., Abramowicz, 2002, astro-ph/0203314
- Kotani T., Ebisawa K., Dotani T., Inoue H., Nagase F., Tanaka Y., Ueda Y., 2000, ApJ, 539, 413
- Kubota A., Done C., 2004, MNRAS, 353, 980
- Kubota A., Makishima K., 2004, ApJ, 601, 428
- Kubota A., Makishima K., Ebisawa K., 2001, ApJ, 560, L147
- Lee J. C., Reynolds C. S., Remillard R., Schulz N. S., Blackman E. G., Fabian A. C., 2002, ApJ, 567, 1102
- Martocchia A., Matt G., Karas V., Belloni T., Feroci M., 2002, A&A, 387, 215
- Martocchia A., Matt G., Karas V., Belloni T., Feroci M., 2004, NuPhS, 132, 404
- McClintock J. E., Shafee R., Narayan R., Remillard R. A., Davis S. W., Li L.-X., 2006, ApJ, submitted, astro-ph/0606076
- McKinney J. C., 2005, ApJ, 630, L5
- McKinney J. C., Gammie C. F., 2004, ApJ, 611, 977
- Merloni A., Fabian A. C., Ross R. R., 2000, MNRAS, 313, 193
- Merloni A., Vietri M., Stella L., Bini D., 1999, MNRAS, 304, 155
- Mitsuda K., et al., 1984, PASJ, 36, 741
- Moderski R., Sikora M., Lasota J.-P., 1998, MNRAS, 301, 142
- Muno M. P., Morgan E. H., Remillard R. A., 1999, ApJ, 527, 321
- Mirabel I. F., Rodríguez L. F., 1994, Natur, 371, 46
- Rodríguez L. F., Mirabel I. F., 1999, ApJ, 511, 398
- Shafee R., McClintock J. E., Narayan R., Davis S. W., Li L.-X., Remillard R. A., 2006, ApJ, 636, L113
- Shakura N. I., Sunyaev R. A., 1973, A&A, 24, 337
- Shimura T., Takahara F., 1995, ApJ, 445, 780
- Sobolewska M. A., Życki P. T., 2003, A&A, 400, 553
- Stella L., Vietri M., 1999, PhRvL, 82, 17
- Strohmayer T. E., 2001, ApJ, 554, L169
- Török G., Abramowicz M. A., Kluźniak W., Stuchlík Z., 2005, A&A, 436, 1
- Zdziarski A. A., Gierliński M., Rao A. R., Vadawale S. V., Mikołajewska J., 2005, MNRAS, 360, 825
- Zdziarski A. A., Johnson W. N., Magdziarz P., 1996, MNRAS, 283, 193
- Zhang S. N., Cui W., Chen W., 1997, ApJ, 482, L155
- Życki P. T., Done C., Smith D. A., 1999, MNRAS, 305, 231